

A. Rakhmatulina¹, A. Altybay², N. Imanbayeva³, A. Moldashev¹

¹ U.A. Joldasbekov Institute of Mechanics and Engineering, Almaty, Kazakhstan

² Institute of Mathematics and Mathematical Modeling, Almaty, Kazakhstan

³ Satbayev University, Almaty, Kazakhstan

E-mail: arshyn.altbay@gmail.com

NUMERICAL SIMULATION OF THE HEAT TRANSFER PROCESS IN VACUUM-SUBLIMATION DRYING

Abstract. In the present investigation, we conduct a comprehensive numerical simulation to explore the complexities of heat and mass transfer phenomena during the vacuum drying process. Specifically, our focus is on the critical third phase of vacuum drying, which incorporates the heating process. To accurately model these phenomena, we employed a sophisticated three-dimensional heat equation, formulated in cylindrical coordinates, that captures the nuanced dynamics of the system. Furthermore, to ensure the reliability and validity of our model, a rigorous stability and accuracy analysis was performed on the finite difference equations utilized in the simulation. The outcomes of this simulation were then meticulously visualized, offering intuitive insights into the heat and mass transfer mechanisms at play during the vacuum drying process. This approach not only enhances our understanding of the drying process but also contributes to the refinement of numerical modeling techniques in the study of vacuum drying systems.

Keywords. Numerical simulation, heat and mass transfer, vacuum drying process, heat equation.

Introduction.

Vacuum-sublimation drying is a crucial process utilized in various industries, including pharmaceuticals, food, and materials science, for the dehydration and preservation of sensitive materials. Unlike conventional drying methods, vacuum-sublimation drying operates under reduced pressure conditions, allowing for the removal of moisture without subjecting the material to high temperatures that could degrade its quality. Understanding the intricacies of heat transfer in vacuum-sublimation drying is paramount for optimizing the process efficiency and product quality. [1–2]. De-spite its advantages, optimizing the drying process to enhance efficiency and product quality remains a challenge due to the complex heat and mass transfer phenomena involved.

Numerical simulation of the heat transfer process in vacuum-sublimation drying is crucial as it enables a detailed understanding and optimization of complex drying processes, leading to improved product quality, cost and time efficiency, and safe process control. By simulating different conditions and parameters, researchers can optimize drying processes, design and scale-up equipment, and innovate new solutions without the high costs and time associated with extensive experimental trials. This enhances efficiency, ensures product consistency, and drives innovation in industries such as food and pharmaceuticals [3].

In the context of vacuum-sublimation drying, numerical simulations enable re-searchers to study the interplay between temperature, pressure, material properties, and geometric configurations, facilitating the design of efficient drying systems. Patel and his colleagues provide an in-depth review of numerical modelling efforts in the context of vacuum drying of

food products, highlighting the challenges and opportunities in accurately simulating the drying process [4].

This paper focuses on the numerical simulation of the heat transfer process in vacuum-sublimation drying within a cylindrical domain. The cylindrical geometry is common in many practical applications, such as drying chambers and vessels, making it an appropriate choice for modelling and analysis. Using numerical methods, we aim to elucidate the heat transfer mechanisms governing the drying process and provide insights into the factors influencing drying rates, uniformity, and energy consumption.

This study builds upon previous research efforts in the field of heat transfer and drying processes. Notable contributions include the work of Mujumdar et al. [5], who investigated convective drying processes and their applications in food and agricultural engineering. Additionally, the comprehensive review by Chen and Mujumdar [6] provides insights into the fundamental principles of drying and the role of numerical simulations in process optimization. Finite difference discretization's in polar or cylindrical coordinates have been used by authors to solve partial differential equations [10-13]. Mori and Romao [8] used the finite difference method to perform numerical simulation of 2D convection-diffusion in cylindrical coordinates. Endalew G. T. [7] used the fourth-order difference method for the solution of 3D convection-heat equation in cylindrical coordinates. In work [14] considered analytical solution and numerical simulation of Heat Transfer in Cylindrical- and Spherical-Shaped Bodies, here the authors used explicit and unconditionally stable finite difference methods.

However, in all these studies, the heat source is treated as a boundary condition of the simulated domain. In reality, the heat source is often an internal heat source located within the domain. Additionally, similar simulations in cylindrical domains have been scarcely explored. Therefore, numerical simulation of heat transfer processes with an internal heat source is crucial.

In this work, we numerically simulate the distribution of heat within a cylindrical domain featuring an internal heat source. Initially, we convert the three-dimensional heat transfer equation in cylindrical coordinates, inclusive of the heat source, into a finite difference equation. We then analyze the stability of the finite difference scheme using the von Neumann stability analysis and assess the accuracy of the scheme through numerical calculations. Subsequently, we perform numerical simulations at various time steps.

Our numerical simulations aim to deepen the understanding of the unique challenges and opportunities associated with vacuum-sublimation drying.

Materials and methods.

The problem at hand involves modeling the heat transfer process within a cylindrical chamber equipped with shelves for holding objects during vacuum-sublimation drying. The cylindrical chamber is typically used in industrial drying applications due to its efficient space utilization and ease of construction. Heat is supplied to the chamber through the shelves, which act as heat sources, thereby facilitating the drying process.

The objective is to develop a mathematical model and numerical solution approach to predict the temperature distribution within the cylindrical chamber and on the shelves during the vacuum-sublimation drying process. Understanding the heat distribution is critical for optimizing drying efficiency, ensuring uniform drying of objects placed on the shelves, and minimizing energy consumption.

Material and Geometry. The layout of the Laboratory Vacuum Dryer is shown in Figure 1.

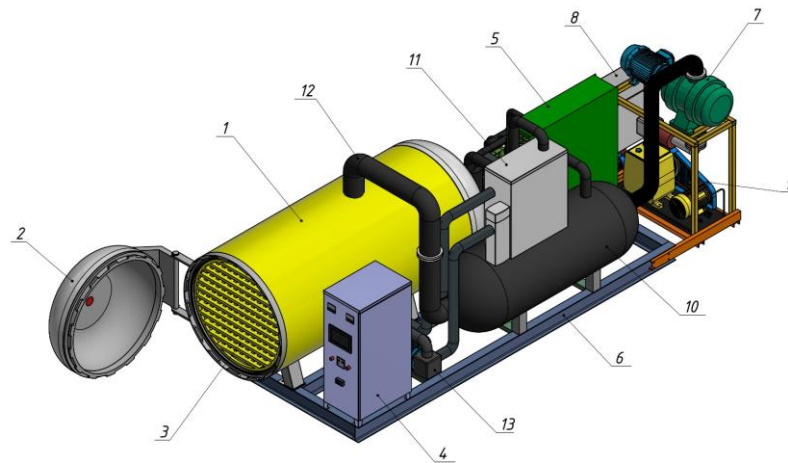


Figure 1 - Vacuum Dryer

Here, 1. Vacuum chamber 2. Vacuum chamber shutter 3. Heated intermediate plates 4. Control panel 5. Compressor condensing unit 6. Base (Frame) 7. Vacuum control system 8. Heat exchanger 9. Compressor 10. Lyophilizer 11. Container for silicone oil 12. Vacuum pipelines 13. Circulation pump.

Items to be dried are placed on shelves inside the vacuum chamber. To maintain a certain level of heat on the shelves, silicone liquid is used, which is distributed inside the shelves using hoses. The interior of the vacuum chamber is depicted in Figure 2, which represents our research area.

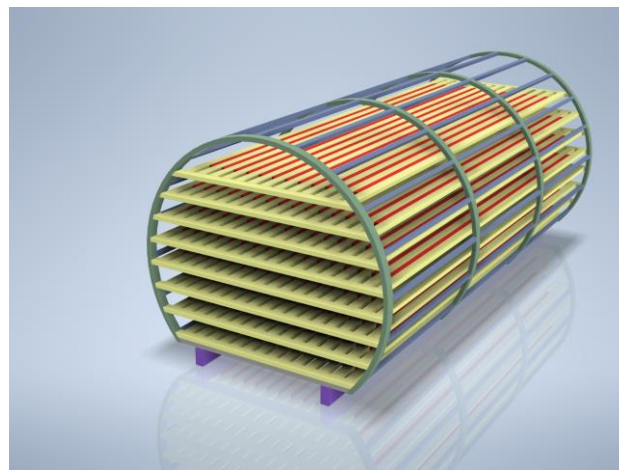


Figure 2 - Inside the vacuum chamber

Governing equations. The governing equation for heat transfer within the cylindrical chamber and shelves can be described by the heat conduction equation in cylindrical coordinates:

$$\rho c \frac{\partial^2 T}{\partial t^2} = \lambda \left[\frac{1}{r} \frac{\partial T}{\partial r} + \frac{\partial^2 T}{\partial r^2} + \frac{1}{r^2} \frac{\partial^2 T}{\partial \theta^2} + \frac{\partial^2 T}{\partial z^2} \right] + Q(t, r, \theta, z) \quad (t, r, \theta, z) \in (0, T) \times \Omega, \quad (1)$$

where T is the temperature distribution, Q is the heat source, r is the radial distance, θ is the azimuthal angle, z is the axial distance, and λ is the thermal diffusivity of the material, ρ is density, c is heat capacity.

Initial conditions involve specifying the initial temperature distribution within the chamber and shelves at the start of the drying process. The initial values are given by the initial value condition

$$T(0, r, \theta, z) = T_0(r, \theta, z), 0 \leq r \leq R, 0 \leq \theta \leq 2\pi, 0 \leq z \leq L, \quad (2)$$

where $\Omega = (0, R) \times (0, 2\pi) \times (0, L)$.

At the outer surface of the cylindrical chamber, adiabatic boundary conditions are typically assumed, representing minimal heat loss to the surroundings. So we can set boundary conditions as a Dirichlet boundary condition

$$u(t, r, \theta, z)|_{\partial\Omega} = 0, t \in [0, T], \quad (3)$$

Finite Difference Discretization and numerical method. For the discretization of 2.5 we consider a uniform mesh $t_n = n\Delta t, n = 0, 1, \dots, M; r_i = i\Delta r, i = 0, 1, \dots, N_r; \theta_j = j\Delta\theta, j = 0, 1, \dots, N_\theta; z_k = k\Delta z, k = 0, 1, \dots, N_z$. The difference equation for (1) is

$$\frac{T_{i,j,k}^{n+1} - T_{i,j,k}^n}{\Delta t} = \alpha \frac{T_{i+1,j,k}^n - T_{i-1,j,k}^n}{r_i \cdot 2\Delta r} + \alpha \frac{T_{i+1,j,k}^n - 2T_{i,j,k}^n + T_{i-1,j,k}^n}{\Delta r^2} + \frac{\alpha}{r_i^2} \frac{T_{i,j+1,k}^n - 2T_{i,j,k}^n + T_{i,j-1,k}^n}{\Delta\theta^2} + \alpha \frac{T_{i,j,k+1}^n - 2T_{i,j,k}^n + T_{i,j,k-1}^n}{\Delta z^2} + Q_{i,j,k}^n, \quad (4)$$

where $T(t, r, \theta, z) = T^n(i, j, k)$, n is the current time index, Δt is the step size for time discretization, and $\Delta r, \Delta\theta$, and Δz are mesh spacing in r, θ , and z directions, α is thermal conductivity, $\alpha = \lambda/\rho c$. Approximation of the finite difference scheme (4) is first-order in time and second-order accurate in spatial derivatives. This finite difference scheme is solved using the Jacobi Iteration method. Grouping similar terms from equation (4), we obtain

$$T_{i,j,k}^{n+1} = T_{i,j,k}^n + \frac{\alpha\Delta t}{2r_i\Delta r} (T_{i+1,j,k}^n - T_{i-1,j,k}^n) + \frac{\alpha\Delta t}{\Delta r^2} (T_{i+1,j,k}^n - 2T_{i,j,k}^n + T_{i-1,j,k}^n) + \frac{\alpha\Delta t}{r_i^2\Delta\theta^2} (T_{i,j+1,k}^n - 2T_{i,j,k}^n + T_{i,j-1,k}^n) + \frac{\alpha\Delta t}{\Delta z^2} (T_{i,j,k+1}^n - 2T_{i,j,k}^n + T_{i,j,k-1}^n) + \Delta t Q_{i,j,k}^n. \quad (5)$$

Results.

Stability analysis. The Von Neumann stability analysis [9] is used to check the stability condition of the numerical method.

Here we perform stability analysis for equation (5). To investigate the stability of the scheme we start with the usual ansatz To conduct the Von Neumann stability analysis and derive the stability criteria for the given finite difference scheme with the source term $Q_{i,j,k}^n$, we start by assuming a solution of the form:

$$T_{i,j,k}^n = G^n e^{i\alpha_r i\Delta r} e^{i\alpha_\theta j\Delta\theta} e^{i\alpha_z k\Delta z}, \quad (6)$$

where G is the amplification factor, and α_r, α_θ , and α_z are the wave numbers in the radial, angular, and axial directions, respectively. Substituting this solution into the finite difference equation (5), we obtain:

$$G = 1 + \frac{\alpha \Delta t}{2} \left(\frac{1}{r_i \Delta r} \right) (\xi_r - 1) + \frac{\alpha \Delta t}{\Delta r^2} (\xi_r - 2 + \xi_r^{-1}) + \frac{\alpha \Delta t}{r_i^2 \Delta \theta^2} (\xi_\theta - 2 + \xi_\theta^{-1}) + \frac{\alpha \Delta t}{\Delta z^2} (\xi_z - 2 + \xi_z^{-1}) + \frac{\Delta t}{G} Q_{i,j,k}^n, \quad (7)$$

where $\xi_r = e^{I\alpha_r i \Delta r}$, $\xi_\theta = e^{I\alpha_\theta j \Delta \theta}$, and $\xi_z = e^{I\alpha_z k \Delta z}$.

To derive the stability criteria, we analyze each term:

- Radial term: $\frac{\alpha \Delta t}{2} \left(\frac{1}{r_i \Delta r} \right) (\xi_r - 1)$

This term contributes to stability regardless of the value of α_r .

- Angular term: $\frac{\alpha \Delta t}{r_i^2 \Delta \theta^2} (\xi_\theta - 2 + \xi_\theta^{-1})$

This term contributes to stability regardless of the value of α_θ .

- Axial term: $\frac{\alpha \Delta t}{\Delta z^2} (\xi_z - 2 + \xi_z^{-1})$

This term contributes to stability regardless of the value of α_z .

- Source term: $\frac{\Delta t}{G} Q_{i,j,k}^n$

For stability, we require $|\frac{\Delta t}{G} Q_{i,j,k}^n| \leq 1$. Since G is the amplification factor, $|G| \leq 1$ or stability. Therefore, we can ensure stability if $\Delta t \leq 17$

Based on the analysis of each term, the stability criteria for the finite difference scheme with the source term $Q_{i,j,k}^n$ are:

$$0 < \Delta t \leq \left\{ \frac{2}{\alpha r_i \Delta r}, \frac{1}{\alpha r_i^2 \Delta \theta^2}, \frac{1}{\alpha \Delta z^2}, \frac{1}{|Q_{i,j,k}^n|} \right\}. \quad (8)$$

These conditions ensure that the amplification factor G remains bounded, ensuring stability for the finite difference scheme with the source term $Q_{i,j,k}^n$

Accuracy analysis. To evaluate the accuracy of the numerical solution obtained using a finite-difference scheme, the maximum error and the L^2 error norm are used. The maximum error (E) and the L^2 error norm are defined as follows:

$$E = \max ||T - T_{num}||$$

$$L^2 = \sqrt{\sum_{i=1}^n (T - T_{num})^2 \Delta r \Delta \theta \Delta z},$$

where T denotes the exact value and T_{num} denotes the approximation.

Consider the following problem with initial and boundary conditions:

$$\frac{\partial^2 T}{\partial t^2} = \frac{1}{r} \frac{\partial T}{\partial r} + \frac{\partial^2 T}{\partial r^2} + \frac{1}{r^2} \frac{\partial^2 T}{\partial \theta^2} + \frac{\partial^2 T}{\partial z^2} \quad 0 \leq r \leq R, 0 \leq z \leq L, 0 \leq \theta \leq 2\pi, t > 0,$$

$$T(0, r, \theta, z) = J_\alpha \left(\frac{s_1 r}{R} \right) (2 \cos(\theta) + 2 \sin(\theta)) \cos(\pi z L) e^{-\alpha \left(\left(\frac{s_1}{R} \right)^2 + \left(\frac{\pi}{L} \right)^2 \right)},$$

$$T(t, R, \theta, z) = 0, T(t, r, \theta, z) = T(t, r, 2\pi, z) = 0, T_z(t, r, \theta, 0) = 0, T_z(t, r, \theta, L) = 0.$$

The analytical solution is as follows

$$T(t, r, \theta, z) = J_\alpha\left(\frac{s_1 r}{R}\right) (2\cos(\theta) + 2\sin(\theta)) \cos(\pi z L) e^{-\alpha((s_1/R)^2 + (\pi/L)^2)t},$$

$$0 \leq r \leq R = 1, 0 \leq z \leq L = 2, 0 \leq \theta \leq 2\pi.$$

where $J_\alpha(x)$ is the Bessel function of the first kind and s_1 is the first positive zero of J_α [7].

Table 1 provides the maximum error and L^2 norm values for different combinations of time and spatial steps

Table 1 - Maximum errors and L^2 norm errors

Δr	$\Delta \theta$	Δz	Δt	Maximum error	L^2 norm
0.01	$\pi/16$	0.1	0.0001	2.45655e-3	1.48964e-3
0.02	$\pi/32$	0.01	0.0005	2.12562e-3	4.38543e-4
0.001	$\pi/64$	0.001	0.00001	1.87473e-3	1.04570e-5
0.0001	$\pi/128$	0.0001	0.00001	1.16898e-3	3.26881e-6

The provided table 1 compares the numerical solution and the analytical solution of the 3-dimensional heat transfer equation in cylindrical coordinates. It presents the results for different discretization parameters ($\Delta r, \Delta \theta, \Delta z$, and Δt), along with the corresponding maximum error and L^2 norm comparison data.

From the table, we can observe the following trends: As the spatial and temporal discretization parameters ($\Delta r, \Delta \theta, \Delta z$, and Δt) decrease, the maximum error and the L^2 norm error tend to decrease. This indicates that using smaller discretization steps leads to a more accurate numerical solution.

The L^2 norm error tends to decrease at a faster rate compared to the maximum error as the discretization parameters decrease. This suggests that the overall solution converges more rapidly in the L^2 norm sense compared to the pointwise maximum error. The choice of discretization parameters significantly affects the accuracy of the numerical solution. Smaller values of ($\Delta r, \Delta \theta, \Delta z$, and Δt) result in more accurate solutions but may require more computational resources.

Discussion.

Consider three-dimensional transient heat conduction which satisfies Equation (5) in a solid cylinder made up of stainless-steel having dimensions $0 \leq r \leq 1, 0 \leq z \leq 1$, and $0 \leq \theta \leq 2\pi$. We will assume that there is no heat exchange with the external environment, and the heat source is located inside the cylinder, as shown in Figure 3.

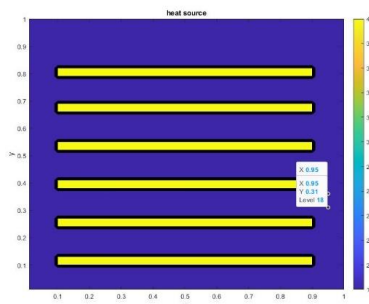


Figure 3- Heat Source

A cross-section of some simulation results is shown in Figure 4.

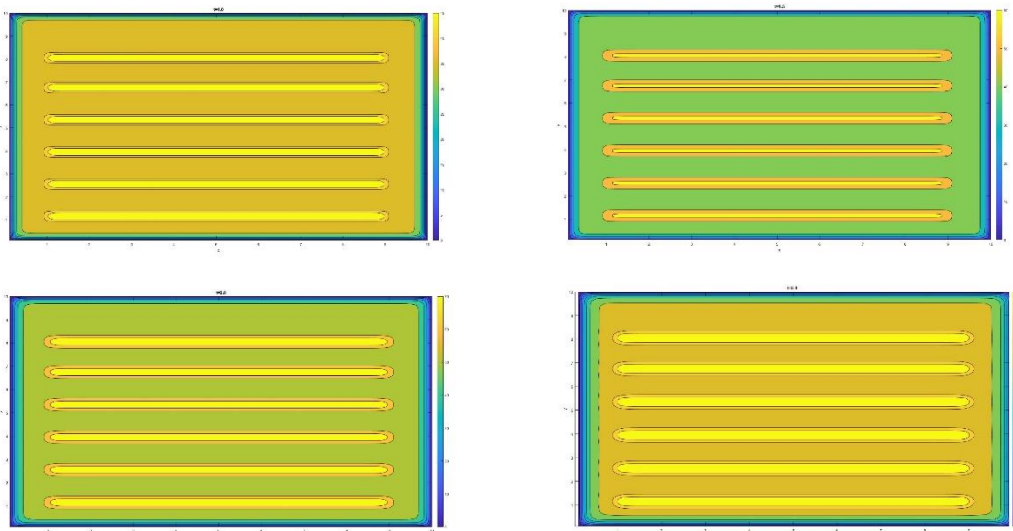


Figure 4 - Temperature distributions at different times

The graphs presented in Figure 4 effectively illustrate the temporal distribution of heat transfer from the heat source within the cylindrical chamber, as obtained from the numerical solution of the three-dimensional heat conduction equation. The cross-section of some simulation results provides a detailed view of the heat distribution at various time intervals, highlighting the dynamic nature of the thermal process.

In our case, the shelves on which the items are to be dried are placed above the heat source, it is possible to predict when the items to be dried will reach the normal drying temperature through such simulations. These visualizations not only confirm the theoretical predictions but also enhance our comprehension of heat behavior in complex geometries, serving as a valuable tool for further analysis and optimization of thermal systems.

Conclusion.

In this paper, a numerical simulation of the heating process, which represents the third stage of vacuum drying, was performed. A finite-difference scheme has been developed for the heat equation in three-dimensional space using cylindrical coordinates. The stability and accuracy of the method were analyzed. The implementation of numerical calculations using a discrete scheme is carried out in the MATLAB environment, which ensures reliable operation and ease of use.

Funding Statement. This research was funded by the Committee of Science of the Ministry of Science and Higher Education of the Republic of Kazakhstan (Grant No. BR21881957).

REFERENCES

- [1] Jennings, T. A. (2020). Principles of Freeze-Drying. *The Pharmaceutical Journal*, 304(7890).
- [2] Liu, F., Zhang, M., and Bhandari, B. (2018). Understanding the Impact of Freeze-Drying on the Structural Quality of Foods. *Critical Reviews in Food Science and Nutrition*, 58(14), 2365-2378.
- [3] Smith, A., and Jones, B. (2019). Advances in Numerical Simulation of the Freeze-Drying Process. *Journal of Thermal Analysis and Calorimetry*, 137(1), 37-45.

[4] Patel, R. K., Robinson, D., and Lee, P. Y. (2021). Numerical Modelling of Heat and Mass Transfer in Vacuum Drying of Food Products. *Food Engineering Reviews*, 13(2), 210-230.

[5] Mujumdar, A.S., Law, C.L., and Chen, X.D. (2017). Drying Technology: Trends and Applications in Postharvest Processing. *Drying Technology*, 35(7), 779-785. [6] Chen, X.D., and Mujumdar, A.S. (2007). Drying Technologies in Food Processing. In *Food Engineering Series* (Vol. 7). Springer.

[7] Endalew G. T. (2022). Numerical Solution of Three-Dimensional Transient Heat Conduction Equation in Cylindrical Coordinates. *Journal of Applied Mathematics*, vol. 2022, Article ID1993151, 8 pages. <https://doi.org/10.1155/2022/1993151>

[8] Mori C. N. T., and Romão E. C. (2015). Numerical simulation by finite difference method of 2D convection-diffusion in cylindrical coordinates, *Applied Mathematical Sciences*, vol. 9, no. 123, pp. 6157–6165

[9] von Neumann, J., and Richtmyer, R. D. (2004) A Method for the Numerical Calculation of Hydrodynamic Shocks, *J. Appl. Phys.*, vol 21, no.3, pp. 232–237.

[10] Yue P., Xiao H., and Xiuming W. (2023) 3D Viscoelastic Finite-Difference Analysis of the Monopole Acoustic Logs in Cylindrical Coordinates. *Journal of Theoretical and Computational Acoustics* Vol. 31, No. 01, 2250006 <https://doi.org/10.1142/S2591728522500062>

[11] Altybay, A., Ruzhansky, M., Tokmagambetov, N. (2020) A parallel hybrid implementation of the 2D acoustic wave equation. *International Journal of Nonlinear Sciences and Numerical Simulation*. Vol.21(7-8), pp.821-8277

[12] Shiferaw A. and Mittal R. C. (2013). Fast finite difference solutions of the three-dimensional Poisson's equation in cylindrical coordinates, *American Journal of Computational Mathematics*, vol. 2013, no. 3, pp. 3056–3361.

[13] Salehi M., Granpayeh N. (2020). Numerical solution of the Schrödinger equation in polar coordinates using the finite difference time-domain method, *Journal of Computational Electronics*, vol. 19, no. 1, pp. 91–1027.

[14] Jalghaf, H. K., Endre K., Imre F. B., and László M. (2023). Analytical Solution and Numerical Simulation of Heat Transfer in Cylindrical- and Spherical-Shaped Bodies *Computation* 11, no. 7: 131. <https://doi.org/10.3390/computation11070131>

Аяулым Рахматулина, PhD, қауымдастырылған профессор, Ө.А. Жолдасбеков атындағы механика және машинатану институты, Алматы, Қазақстан, kazrah@mail.ru

Аршын Алтыбай, PhD, Математика және математикалық модельдеу институты, Алматы, Қазақстан, arshyn.altybay@gmail.com

Нұрбибі Иманбаева, т.ғ.к., Satbayev University, Алматы, Қазақстан, imanbaevan@mail.ru

Арман Молдашев, кіші ғылыми қызметкер, Ө.А. Жолдасбеков атындағы механика және машинатану институты, Алматы, Қазақстан, armanmoldashev@gmail.com

ВАКУУМДЫ-СУБЛИМАЦИЯЛЫҚ КЕПТІРУДЕ ЖЫЛУ АЛМАСУ ПРОЦЕСІН САНДЫҚ МОДЕЛЬДЕУ

Аңдатпа. Осы зерттеуде біз вакуумда кептіру процесі кезінде жылу және масса алмасу құбылыстарының күрделілігін зерттеу үшін жан-жақты сандық модельдеу жүргіземіз. Атап айтқанда, біздің назарымыз қыздыру процесін қамтитын вакуумда кептірудің маңызды үшінші кезеңіне бағытталған. Бұл құбылыстарды дәл модельдеу үшін біз цилиндрлік координаттарда тұжырымдалған, жүйенің нюансты динамикасын қамтитын күрделі үш өлшемді жылуөткізгіштік теңдеуін қолдандық. Сонымен қатар, модельміздің сенімділігі мен негізділігін қамтамасыз ету үшін модельдеуде қолданылған

ақырлы айырмдылық теңдеулеріне тұрақтылық пен дәлдік талдаулары жасалды. Содан кейін бұл модельдеу нәтижелері мұқият визуалды түрде көрсетілді, бұл вакуумда кептіру процесінде туындайтын жылу және масса алмасу механизмдері туралы интуитивті түсініктерді ұсынады. Бұл тәсіл кептіру процесі туралы түсінігімізді кеңейтіп қана қоймай, сонымен қатар вакуумда кептіру жүйелерін зерттеуде сандық модельдеу әдістерін жетілдіруге ықпал етеді.

Түйінді сөздер. Сандық модельдеу, жылу және масса алмасу, вакуумда кептіру процесі, жылуөткізгіштік теңдеуі.

Аяулым Рахматулина, PhD, ассоциированный профессор, Институт механики и машиностроения имени У. А. Джолдасбекова, Алматы, Казахстан, kazrah@mail.ru

Аршын Алтыбай, PhD, Институт математики и математического моделирования, Алматы, Kazakhstan, arshyn.altybay@gmail.com

Нұрбибі Иманбаева, к.т.н., Satbayev University, Алматы, Казахстан, imanbaevan@mail.ru

Арман Молдашев, младший научный сотрудник, Институт механики и машиностроения имени У. А. Джолдасбекова, Алматы, Казахстан, armanmoldashev@gmail.com

ЧИСЛЕННОЕ МОДЕЛИРОВАНИЕ ПРОЦЕССА ТЕПЛОПЕРЕДАЧИ ПРИ ВАКУУМНО-СУБЛИМАЦИОННОЙ СУШКЕ

Аннотация. В настоящем исследовании мы проводим комплексное численное моделирование для изучения сложностей явлений тепло- и массопереноса в процессе вакуумной сушки. В частности, мы сосредоточены на важнейшем третьем этапе вакуумной сушки, который включает в себя процесс нагрева. Чтобы точно смоделировать эти явления, мы использовали сложное трехмерное уравнение теплопроводности, сформулированное в цилиндрических координатах, которое отражает тонкую динамику системы.

Кроме того, чтобы гарантировать надежность и достоверность нашей модели, был проведен строгий анализ устойчивости и точности конечно-разностных уравнений, используемых в моделировании. Результаты этого моделирования были затем тщательно визуализированы, что дало интуитивное представление о механизмах тепло- и массопереноса, действующих в процессе вакуумной сушки. Этот подход не только расширяет наше понимание процесса сушки, но и способствует совершенствованию методов численного моделирования при исследовании систем вакуумной сушки.

Ключевые слова. Численное моделирование, тепломассоперенос, процесс вакуумной сушки, уравнение теплопроводности.

Редакцияға түсті / Поступила в редакцию / Received 31.05.2024

Жариялауға қабылданды / Принята к публикации / Accepted 24.09.2024